31st Int. Linear Accel. Conf. LINAC2022, Liverpool, UK JACoW Publishing
ISBN: 978-3-95450-215-8 ISSN: 2226-0366 doi:10.18429/JACoW-LINAC2022-MOPOPA15

Content from this work may be used under the terms of the CC BY 4.0 licence (© 2021). Any distribution of this work must maintain attribution to the author(s), title of the work, publisher, and DOI

3 YEARS OF OPERATION OF THE SPIRAL2 SC LINAC - RF FEEDBACK

M. Di Giacomo†, M. Aburas, P-E. Bernaudin, O. Delahaye, A. Ghribi, J-M. Lagniel,
J-F. Leyge, G. Normand, A.K. Orduz, F. Pillon, L. Valentin, A. Dubosq, GANIL, Caen, France
F. Bouly, LPSC, Université Grenoble-Alpes , CNRS/IN2P3, Grenoble , France
S. Sube, CEA-DRF-IRFU, Saclay, France

Abstract

The superconducting LINAC of SPIRAL2 at the GANIL facility has been in operation since October 2019. The accelerator uses 12 low beta and 14 high beta superconducting quarter wave cavities, cooled at 4°K, working at 88 MHz. The cavities are operated at a nominal gradient of 6.5 MV/m and are independently powered by a LLRF and a solid-state amplifier, protected by a circulator. Proton and deuteron beam currents can reach 5 mA and beam loading perturbation is particularly strong on the first cavities, as they are operated at field levels much lower than the nominal one.

This paper presents a feedback after three years of operation, focuses on the RF issues, describing problems and required improvement on the low level, control and power systems.

RF SYSTEM DESCRIPTION

The SPIRAL2 accelerator [1] uses independently phased RF cavities, operated at 88.0525 MHz, to accelerate a multitude of ion beams within wide intensity and energy ranges (up to 5 mA and from 0.75 to 20 MeV/A).

Table 1: Main cavity parameters @ opt beta

Parameter	β = 7%	β = 12%
Eacc (MV/m)	6.5	6.5
Field integral (MV)	1.56	2.66
5mA beam loading (kW)	7	12
Qext	$5.5{\cdot}10^5$	$1.1{\cdot}10^6$

The SC LINAC cavities [2] are quarter wave resonators (QWR), hosted in two families of cryomodules (CM). The 12 low beta ones host one QWR each, while the high beta CMs host a couple of QWR each. Table 1 gives the main parameters for both type of cavities.

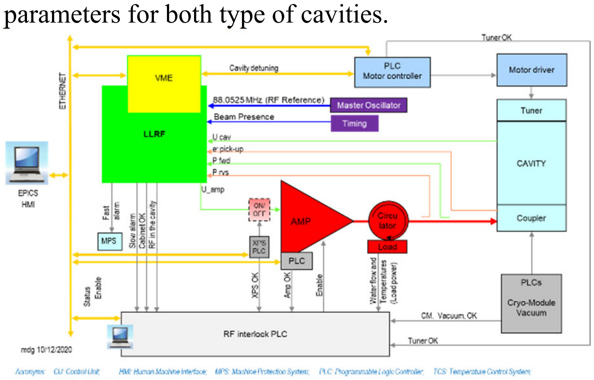

Figure 1: SC cavity RF system block diagram.

† digiacomo@ganil.fr

Each cavity has its own RF system equipped with digital LLRF, solid state amplifier (SSA) and circulator as shown in Fig. 1.

Reference and timing signals are provided by two subsystems: the master oscillator (MO) with its distribution line and the timing electronics (ECSF in the picture). The circulators are installed out of the LINAC tunnel but as near as possible to the cavities, and each system has two sections of transmission lines: TL1 and TL2, the second being designed to withstand strong mismatched conditions (high VSWR).

Commissioning of the first beams took the first three years of operation, and showed several issues that had not arisen during the RF equipment commissioning or that had been insufficiently addressed during the design phase.

CALIBRATIONS

Calibration of the accelerating field amplitudes (Eacc) and of the external Q factors (Qext) was one of the first tasks to check whether it would have been possible to accelerate all ion species at nominal current and energy. That was particularly important for the first low beta cavities, which are used at much lower fields and are driven by 2.5 kW (cavity 1 to 6) and 5 kW (7 to 9) amplifiers (with respect to 10 kW for the last ones and to 19 kW for the high beta cavities).

Eacc

Cavity probes and LLRF acquisition channels had been characterised on the test benches while cables and attenuators had been measured in situ, after installation. Nevertheless, during the acceleration of the first beams showed that most of the cavity fields were over-estimated (see Fig. 2).

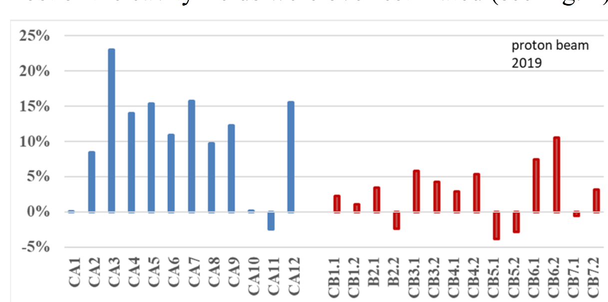

Figure 2: field error before calibration.

The accelerating fields were then calibrated looking at the effect of the first proton beam on each single cavity. Smaller corrections have followed, while accelerating various beam species and improving the measurement methods.

ISBN: 978-3-95450-215-8 ISSN: 2226-0366 doi:10.18429/JACoW-LINAC2022-MOPOPA15

Qext

Qext is one of the main parameters contributing to the RF power requirements, and one of the most delicate and time consuming to measure. For each cavity, it has been calculated from the Eacc exponential decay time constant and from RF power measurement as shown in Fig. 3 for the low beta family, where the shadowed area represents the range initially defined by the acceptance criteria.

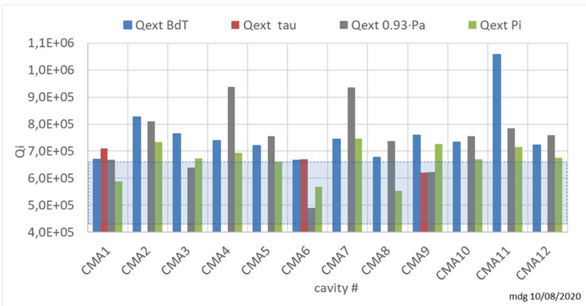

Figure 3: Qext estimation by different methods. Bdt and tau: Eacc exponential decay respectively at 1 MV/m, (performed during the test bench commissioning of each cavity) and at 6.5 MV/m performed at GANIL after installation and cool-down), 0.93·Pa and Pi: RF power indicated by the amplifier (corrected by a factor of 7% loss in the circulator and transmission lines) and by the directional coupler at the cavity entrance.

SUBSYSTEM FEEDBACK

Master oscillator (+ RF reference distribution)

This subsystem is shown in Fig. 4 and is briefly introduced as it is not described elsewhere, while a more detailed description of the LLRF and the amplifiers can be found in references [3, 4].

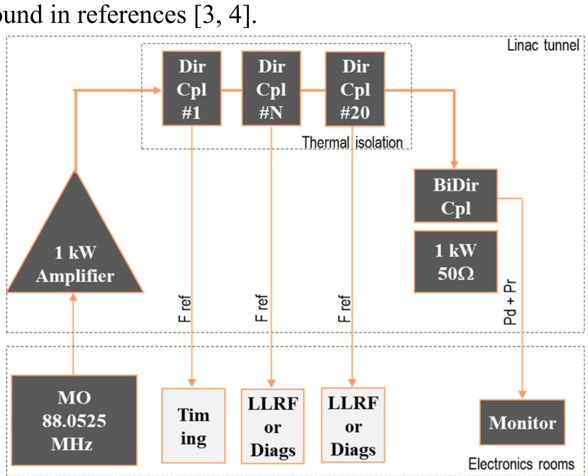

Figure 4: MO and reference distribution bloc diagram.

The master oscillator is derived from a commercial FM modulator. As shown in Fig. 5, the central frequency is 88.05248 MHz, and the spectral purity is better than 43 dBc. The slow drift is 10^{-6} Hz/year.

The amplifier is a commercial 1kW device providing stabilized output power: ±0.2° in phase and ±0.2 dB in amplitude. It is operated at 550 W (~50W reflected) into a 7/8" transmission line that runs parallel to the LINAC. A thermal screen envelops a water pipe kept at 26°C ±0.2°C and the coaxial line whose temperatures is stable around 32°C, almost independently from the LINAC tunnel thermal conditions. Several directional couplers provide reference signal to the LLRF and diagnostics cabinets at levels up to 23 dBm. For each device, the RF reference and signal cables have almost the same length and follow the same path to compensate differential losses and thermal phase drift. The line is ended on a matching resistor and a bidirectional coupler monitors direct and reverse power on the load.

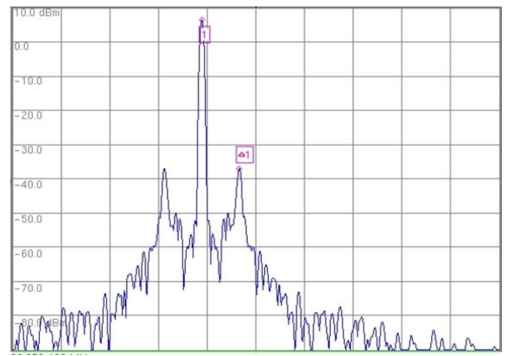

Figure 5: Spectral analysis of the master oscillator driver, with 1 Hz resolution and video bandwidths.

The system has proven to be reliable and stable and no issues arose with it.

Timing

The beam macrostructure (beam pulse) is created via a chopper located in the low energy beam transport (LEBT) and beam power is ramped changing the pulse duty factor. The chopper trigger is generated by the timing system, which can also provide a short pulse turning-off the RFQ for a few milliseconds, to take away the initial beam portion that is affected by space charge compensation (but this is no more used as no effect was visible on beam loss). The pulse repetition rate was around 1 Hz at the beginning of the commissioning but loss monitoring has shown no significant increase at least up to 100 Hz, and higher rates are progressively being used to improve the diagnostics resolution. Timing signals derived from the chopper trigger are used by the LLRF to apply feed-forward (FF) and by the diagnostics.

Digital LLRF

The LLRF uses I and Q feedback (FB) loops and FF to stabilize the accelerating field.

Each loop can be independently tuned thanks to separate PI (Proportional/Integral) controllers. However, the current configuration uses the same proportional (kp) and integral (ki) coefficients for both loops of all the cavities of the same family. Both cavity systems are simulated with Matlab/Simulink [5] and values around kp=75 and ki=0.1 have been set to compensate the beam loading perturbations. Strong FB alone was still not enough for all the cavities because the first ones (which work at much lower voltage) are much more affected as the energy absorbed by the

Content from this work may be used under the terms of the CC BY 4.0 licence (© 2021). Any distribution of this work must maintain attribution to the author(s), title of the work, publisher, and DOI

ISBN: 978-3-95450-215-8 ISSN: 2226-0366 doi:10.18429/JACoW-LINAC2022-MOPOPA15

© Content from this work may be used under the terms of the CC BY 4.0 licence (© 2021). Any distribution of this work must maintain attribution to the author(s), title of the work, publisher, and DOI

beam is a larger fraction of the stored one. FF was eventually added to achieve field stability within the required 1%, 1° range, as shown in Fig. 6. The FF algorithm stores both values of the IQ modulator control signals at the end of each pulse and applies them at the beginning of the next one. We are still trying to optimize the delay between the "beam present" trigger and the FF application, but the field stability has already been improved by a factor of 3 and already fits the requirements.

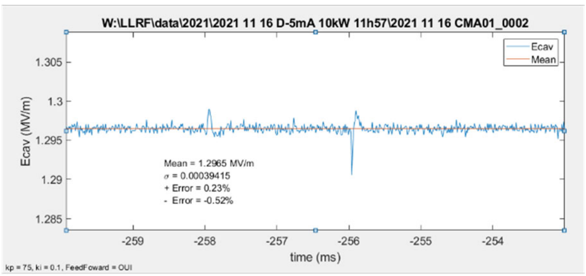

Figure 6: residual field perturbation on cavity A1 with a 5 mA deuteron beam, strong FB and FF. The vertical plot scale is ±1% of the mean value

The LLRF also manages some of the RF protections. It biases the cavity coupler pickup and monitors the electron current Ie^-. The initial Ie^- threshold at which the LLRF was asked to stop the power, was around 130 µA. This value had been established on the basis of the maximum electron current levels observed during the coupler conditioning, which is performed at variable power level and in full mismatched conditions [6]. Beam loading changes the matching conditions and this can generate currents much higher than the ones processed, especially for the cavities operated at low field, then driven with low power level as multipactor (MP) is only observed up to < 100 W in the SPIRAL2 couplers. When strong current (hundreds of µA) arose during the transient edges only, the RF trip was generated by the Ie^- protection but no effect was visible on the vacuum pressure. When the current stays during the whole pulse length, few tens of µA are already enough to trigger a vacuum trip. This behaviour shows that the electron current alone is not (at least in our case, where the RF power in the line is low) representative of the amount of energy associated to the MP or of the ceramic window damage risk. The vacuum pressure being already sensitive enough to protect the window, the Ie^- threshold has been set at 1.6 mA.

Power Amplifiers

The 26 solid state amplifiers are based on 2.5 kW units, used alone, or combined to achieve 5, 10 and 19 kW amplifiers. Each amplifier has its own hardware/microprocessor that runs the protection logic/ algorithms, while a central PLC manages the whole switch on/off procedures and the communication to the main control system.

Three main issues arose since the beginning of operation:

- drift of the transistor quiescent current due to insufficient thermal stability of the bias circuit components,
- too long polling time for the operating parameters (voltages, currents, output powers, etc)
- and unreliable contact of the input connectors final combiners (10 and 20 kW devices).

Solving these problems requires major changes and the issues are not yet fixed on all amplifiers. Some RF modules with new bias circuits have been successfully tested. A new control architecture is being studied and more intermediate diagnostic signal are being installed to prevent damaging the combiners.

The 10 and 19 kW amplifiers were used at their nominal power and in continuous mode during the coupler conditioning phases only. As we don't see any processing effect beyond 100 W, we have reduced by 20% the maximum power level during these processes.

Circulators

The circulators (12x10 kW + 14x20 kW) behave very reliably by the RF point of view, but dirt in the cooling system originates frequent trips and the filters need continuous maintenance. One of the 20 kW units required to be replaced but, as the cavity of that station had been more difficult to start since the beginning, we consider the circulator was damaged during the reception tests and the issue worse during the first years of operation, until destruction.

Transmission lines

The interesting issue with the transmission line is the feedback on the section between the circulators and the high beta cavities. This portion withstands very high mismatching at almost full power (19 kW) during the coupler conditioning phases and is made of 3 $^{1/8}$" standard coaxial lines, with Cu inner tube and Al outer one. At 88 MHz this standard should withstand 63 kW @VSWR=1 but the power level decreases quickly in mismatched conditions. We experienced one trouble at the entrance of cavity B# coupler, at almost λ/4 distance from the antenna tip, likely initiated by thermal untightening of the inner coaxial contact of an elbow. Here again, derating the amplifier should help avoiding future damage.

CONCLUSION

The SC linac RF system has been running since 2017 and experienced few significant problems since then. In two occasions RF issues affected the beam characteristics during a whole run duration, mainly due to lack of spare parts. Work is going on to improve the reliability and control of the amplifiers and to complete the spare stock.

REFERENCES

[1] A. K. Orduz et al., "Commissioning of a high power linac at GANIL: Beam power ramp_up", Phys. Rev. Accel. Beams, 25, 060101. doi : 10.1103/physrevaccelbeams.25.060101

[2] R. Ferdinand, "The SPIRAL2 superconducting linac", in *Proceedings of the PAC09 Conference*, Vancouver, Canada, paper FR2GRIO2.

ISBN: 978-3-95450-215-8 ISSN: 2226-0366 doi:10.18429/JACoW-LINAC2022-MOPOPA15

[3] Ph De Antoni *et al.,* “The architecture of the LLRF electronics for SPIRAL2”, in *Proceedings of the LLRF07 Workshop*, Oak Ridge, Tennessee, Oct 2007.

[4] M. Di Giacomo, “Acceptance tests for the Spiral2 SC Linac RF Power Systems” in *Proc. IPAC13*, Shanghai , China, May 2013, paper WEPFI002.

[5] F. Bouly *et al* , “Superconducting cavity and RF control loop model for the SPIRAL2 linac”, presented at LINAC’22, Liverpool, UK, August 2022, paper THPOPA13, this conference.

[6] P.E. Bernaudin *et al* , “3 years of operation of the SPIRAL2 superconducting Linac, Cryogenics feedback”, presented at LINAC’22, Liverpool, UK, August 2022, paper TUPOGE002, this conference .

© Content from this work may be used under the terms of the CC BY 4.0 licence (© 2021). Any distribution of this work must maintain attribution to the author(s), title of the work, publisher, and DOI